Group IV Photonic Slot Structures for Highly Efficient Gas Sensing in mid-IR

Vittorio M. N. Passaro, Benedetto Troia
Photonics Research Group, DEE
Politecnico di Bari
Via E. Orabona n. 4, 70125 Bari, Italy
e-mail: passaro@deemail.poliba.it
e-mail: ing.b.troja@gmail.com

Francesco De Leonardis
Photonics Research Group, DIASS
Politecnico di Bari
Viale del Turismo n. 8, 74100 Taranto, Italy
e-mail: f.deleonardis@poliba.it

***Abstract*—In this paper, novel high-performance group IV photonic structures for very efficient gas sensing are presented. Various combinations of group IV materials and alloys based on silicon (Si), germanium (Ge), tin (Sn) and carbon (C), have been studied in CMOS-compatible technology for design of optical slot waveguides for homogeneous optical sensors in mid-IR (3.39 µm). An analysis of fabrication tolerances is presented and a comparison among different photonic sensing structures is also given. Theoretical investigation demonstrates very efficient optical field concentrations in the sensing area, as well as ultra high sensitivity of gas sensing for environmental applications.**

Keywords- Silicon-on-Insulator; Photonic Sensors; Gas Sensing; Slot Waveguides; Group IV materials.

I. INTRODUCTION

Nowadays, increasing interest is devoted to photonic label-free integrated sensors and biosensors, which represent the state of the art in a number of application fields, including environmental monitoring, biomedical, healthcare, pharmaceuticals, homeland security, to name a few. Gas sensing is a crucial application field for environment monitoring and health. Usually, spectroscopic-based sensing techniques are used, but with high costs. Both miniaturization, integration and low cost should be possible by photonic structures. However, the integration of photonic devices for gas sensing in sophisticated architectures like Mach-Zehnder interferometers, photonic crystals [1] and ring resonators [2] is not yet developed as for chemical and biochemical sensors [3] [4].

Slot waveguides implemented in Si/SiO_2 material system (Silicon-on-Insulator, SOI) constitute an intriguing photonic sensing approach, which potentially enables high sensitivity (S) and ultra-low limit of detection (LOD) [5]. Optimized SOI slot waveguides designed at λ = 1.55 µm, have been presented in literature [6], demonstrating a homogeneous sensitivity S_h > 1. In order to detect the exact gas concentration, different research groups have proposed some test methods, including spectroscopic absorption, photo-acoustics and electrochemistry. Despite this potential, early mid-IR sensing applications were limited to specific applications due to the involved instrumentation sizes and limited availability of appropriately compact mid-IR optical components, such as light sources, detectors, waveguides and spectrometers. On the other hand, reasons that encourage research efforts in mid-IR gas sensing are mainly related to increasing attention to harmful gases like carbon dioxide (CO_2), carbon monoxide (CO), methane (CH_4) and sulfure dioxide (SO_2), to name a few, all having refractive indices around 1. Moreover, these gases are characterized by absorption spectra in mid-IR, specifically in the range 2-8 µm. Thus, ingenious design techniques are needed to extend group IV photonics from near-IR to mid-IR wavelength range, exploiting the advantages of photonic architectures in terms of high compactness, high sensitivity and low LOD. In this context, this paper presents some significant results for design of efficient group IV photonic sensors working in mid-IR. In particular, several alloys characterized by precise compositional space configurations have been considered in order to ensure optical transparency and prevent photon absorption at λ = 3.39 µm. In addition, optical properties of alloys as SiGeSn, SiGe, SiGeC, GeC and GeSn, have been evaluated by using Sellmeier dispersion equations, in order to predict their refractive indices (RIs) as a function of optical wavelength. In this paper, novel vertical slot waveguides are investigated at 3.39 µm, by using full-vectorial 2D Finite Element Method (FEM) approach [7]. In FEM mesh generation for effective index and modal profile calculation, triangular vector-elements have been adopted with about 35,000 elements and a domain region area of 9 μm^2, using Dirichlet boundary condition. Changing from a perfect electric to a perfect magnetic conductor, influence on simulation results appears to be negligible. In all simulations, the buried oxide layer is assumed 1 µm thick. The influence of slot waveguide geometrical parameters (gap region g, slot height and width of lateral wires w) is analyzed in order to optimize both field confinement in the slot region and homogeneous sensitivity. A detailed optimization to achieve the best alloys of group IV materials enabling ultra-high gas sensing is given. Finally, an analysis of fabrication tolerances is presented.

II. HOMOGENEOUS AND SURFACE SENSING IN OPTICAL SLOT WAVEGUIDES

Slot waveguides represent a very interesting and promising architecture for photonic sensing. In fact, using

 ISBN: 978-1-61208-145-8

such structures it is possible to confine an extremely high optical field in a low RI region called "slot region". In Figure 1, schematic cross-sectional view of a typical slot waveguide is shown. The structure consists of a thin low-index (n_L) slot embedded between two high-index (n_H) regions (Si-wires), separated to each other by a slot region gap g. Due to the large index contrast at the interfaces, the normal electric field undergoes a large discontinuity, which results in a field enhancement in the low-index region [8]:

$$|E_L| = \left(\frac{n_H}{n_L}\right)^2 |E_H| \qquad (1)$$

In Eq. (1) E_L is the E-field in the slot region, while E_H is the E-field in high index regions (Si-wires). Thus, the larger the refractive index contrast ($\Delta n = n_H - n_L$) between slot region and Si-wires, the higher the field confinement in slot region. For instance, an optimized SOI waveguide has been designed at 1.55 µm with $n_{Si} = 3.45$, $n_{SiO2} = 1.45$, and $\Delta n = 2$ [4].

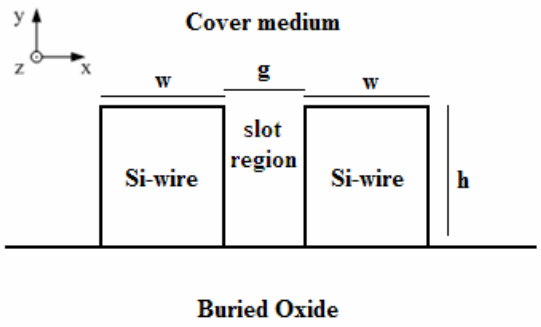

Figure 1. Cross-section of a typical SOI single-slot waveguide.

In vertical slot waveguides, the main E-Field component undergoing discontinuities is that along x-direction, the only one subjected to a refractive index change in the slot region. For this reason, the only fundamental eigenmode considered in this paper is quasi-TE, as shown in Figure 2 for air cover.

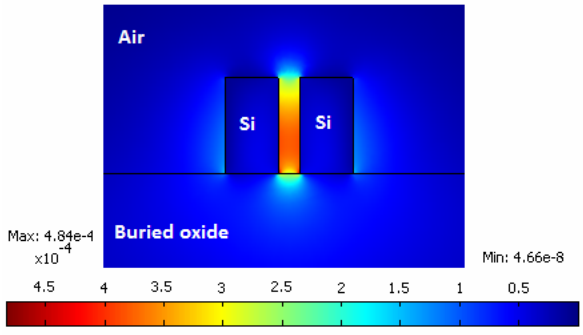

Figure 2. E_x-Field intensity of quasi-TE mode distribution (w = 180 nm, h = 324 nm, g = 70 nm, λ = 1.55 µm, air cover).

Thus, in the design of novel photonic slot waveguides working in mid-IR, high index contrast is needed in order to ensure high E_x-Field confinement. This constitutes a fundamental requirement for both homogeneous and surface sensing. In fact, in both approaches the concentration change of an analyte (gas) to be sensed affects the propagating mode effective index to be monitored in different ways, i.e., reflection, transmission, absorption and so on, according with sensor architecture. In general, this effective index change can be produced either by a change of cover medium refractive index (*homogeneous sensing*) or by a change of thickness of an ultra-thin layer of receptor molecules, immobilized on the waveguide surface (*surface sensing*), as sketched in Figure 3. The ultra-thin adlayer directly influences the mode effective index. As a consequence, it is possible to define two different waveguide sensitivities, one for homogeneous sensing (S_h) and the other for surface sensing (S_s), as follows:

$$S_h = \frac{\partial n_{eff}}{\partial n_c} \qquad S_s = \frac{\partial n_{eff}}{\partial \rho} \qquad (2)$$

where n_{eff} is the propagating mode effective index, n_c is the cover medium RI, and ρ is the molecular adlayer thickness.

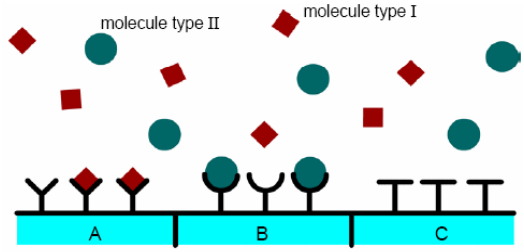

Figure 3. Selective surface sensing of two different types of molecules.

Now, our approach to photonic gas sensing can be classified as homogeneous sensing. In fact, when a particular gas (e.g., CO_2, CO, CO_4, SO_2) covers the device, the cover medium RI will change with respect to air RI as evaluated at the same wavelength. By this way, the index contrast $\Delta n = n_H - n_L$ at the interface between wires and cover medium (gas) will change and, consequently, the optical field distribution in the slot region will be modified according to Eq. 1. Then, its sensitivity S_h can be evaluated as follows [6]:

$$S_h = \left.\frac{\partial n_{eff}}{\partial n_c}\right|_{n_c = n_c^0} = \frac{2 \cdot n_c^0}{\eta_0 \cdot P} \iint_C \left|\vec{E}(x,y)\right|^2 dxdy = \frac{2 \cdot n_c^0 \cdot \Gamma_c}{\eta_0 \cdot P} \iint_\infty \left|\vec{E}(x,y)\right|^2 dxdy \qquad (3)$$

$$P = \iint_\infty \left[\left(\vec{E} \times \vec{H}^* + \vec{E}^* \times \vec{H}\right) \cdot \hat{z}\right] dxdy$$

where n_c^0 is the unperturbed value of n_c, η_0 is the free space impedance (377 Ω), z the unit vector of the propagation direction, and $\vec{E}, \vec{H}$ the electric and magnetic field vectors, respectively. Moreover, optical power confinement factors are defined as the fractions of power confined and guided in the regions of interest, i.e., cover medium including slot (Γ_C) or only slot region (Γ_S), as follows:

 ISBN: 978-1-61208-145-8

$$\Gamma_C = \frac{\iint_C |E(x,y)|^2 \, dxdy}{\iint_\infty |E(x,y)|^2 \, dxdy} \quad (4)$$

$$\Gamma_S = \frac{\iint_S |E(x,y)|^2 \, dxdy}{\iint_\infty |E(x,y)|^2 \, dxdy} \quad (5)$$

where the integrals are calculated in the regions of interest, cover *C* and slot *S*, respectively.

Slot wires are characterized by different combinations of group IV material systems, which have been chosen on the basis of their electronic and optical properties, as well as their technological compatibility.

III. OPTIMIZED GROUP IV OPTICAL SLOT WAVEGUIDES

The first step needed for optimization of these novel group IV photonic sensors is the definition of their alloys and material systems for slot wires. In Table I all group IV materials and alloys employed in this paper are summarized with their refractive indices calculated at 3.39 μm.

TABLE I. GROUP IV ALLOYS AND MATERIALS AND RELEVANT RI

Group IV materials and alloys	RI @ 3.39 μm
Si	3.429
Ge	4.035
SiO_2	1.488
$Si_{0.15}Ge_{0.85}$	3.9441
$Si_{0.08}Ge_{0.91}C_{0.01}$	3.97
$Ge_{0.97}C_{0.03}$	3.9854
$Ge_{0.91}Sn_{0.09}$	4.2340
$Ge_{0.78}Si_{0.08}Sn_{0.14}$	4.2960

At mid-IR wavelengths, it is very important to analyze and ensure very low propagation losses. In fact, the longer the wavelength, the greater the spatial distribution of the E-Field in the guided region and, possibly, the relevant losses. However, it is clear that a percentage of the total confined optical field will interact and be distributed into the buried oxide layer. A lot of investigations have been carried out in order to predict propagation losses of different well known technologies, e.g., SOI, silicon-on-sapphire (SOS) [9]. In particular, using linear interpolation and assuming that a significant fraction (30%) of the guided-mode power is found in the buried insulator layer, the estimated wavelength region with propagation losses less than 2 dB/cm ranges from 1.2 μm to 3.6 μm for SOI (apart from a 2.6÷2.8 μm spike), and from 1.2 μm to 4.3 μm for SOS. Obviously, in order to prevent high propagation losses, it is needed to confine a high percentage of E_x-Field in the slot region instead of dispersing it in the buried oxide.

Additional criteria have been followed for choice of material systems used in this work. In fact, Ge-on-Si exhibits infrared wavelength ranges of operation (1.9 ÷ 16.8 μm and 140 ÷ 200 μm) at 300 K, where the fundamental mode propagation loss is less than 2 dB/cm. The other material system SiGe-on-Si exhibits operative wavelength ranges 1.6 ÷ 12 μm and 100 ÷ 200 μm. Finally, the material system GeSn-on-Si has propagation losses lower than 2 dB/cm in the range 2.2 ÷ 19 μm. Therefore, the principal operative limitation is represented by SiO_2 buried cladding layer, since this layer presents significant propagation losses in a shorter wavelength range.

The optimization procedure proposed in this paper consists in a numerical iterative method allowing to achieve the optimal geometrical configuration giving maximum sensitivity and low losses. This procedure has been applied to each proposed photonic structure, characterized by a different group IV material combination. In Figure 4 cross sectional views of all investigated photonic slot waveguides are sketched. The photonic structures proposed in this paper include Ge-on-Si material system (Figure 4a), SiGe alloy directly grown on SiO_2 (Figure 4b), binary alloy SiGe grown on Si (Figure 4c), SiGeC ternary alloy directly grown on SiO_2 (Figure 4d) and SiGeC-on-Si material system (Figure 4e). Moreover, the last two structures are characterized by slot wires with three different layers, based on SiGeSn-on-GeSn-on-Si (Figure 4f) and SiGeSn-on-GeC-on-Si material system (Figure 4g), respectively.

In Table II all waveguide configurations are named with a letter from (a) to (g) as in Figure 4, in order to simplify the notation. In particular, all alloys and material systems in Figure 4 and Table II are characterized by different percentages of single group IV materials, according with data in Table I. Moreover, optimized parameters are given in Table II, with the only exception of the slot region width *g,* which is considered as a variable for parametric sweep analysis, since it critically influences sensing performance such as sensitivity and confinement factors.

TABLE II. OPTIMIZED GEOMETRICAL STRUCTURES AT λ = 3.39 μm.

	Geometrical parameters [nm]			
Structure	***w***	***h***	***t***	***s***
Type (a)	410	660	40	0
Type (b)	400	690	0	0
Type (c)	400	680	50	0
Type (d)	400	710	0	0
Type (e)	400	690	30	0
Type (f)	380	520	20	50
Type (g)	390	560	20	50

IV. SENSING PERFORMANCE

As stated before, performance parameters, in particular sensitivity S_h and confinement factors Γ_C and Γ_S, have been investigated as a function of the slot region width *g* in each optimized slot waveguide reported in Table II.

In Figure 5 it is possible to note the high value of sensitivity evaluated, being $S_h > 1$ in every structure with $g < 110$ nm. A value $S_h > 1$ clearly implies that an effective index change $\Delta n_{eff} > \Delta n_C$ is induced by a cover index shift Δn_C. The waveguides previously indicated with letters (f) and (b) are the best suitable, because their sensitivities are very high still remain stable over a large range, $g < 140$ nm.

 ISBN: 978-1-61208-145-8

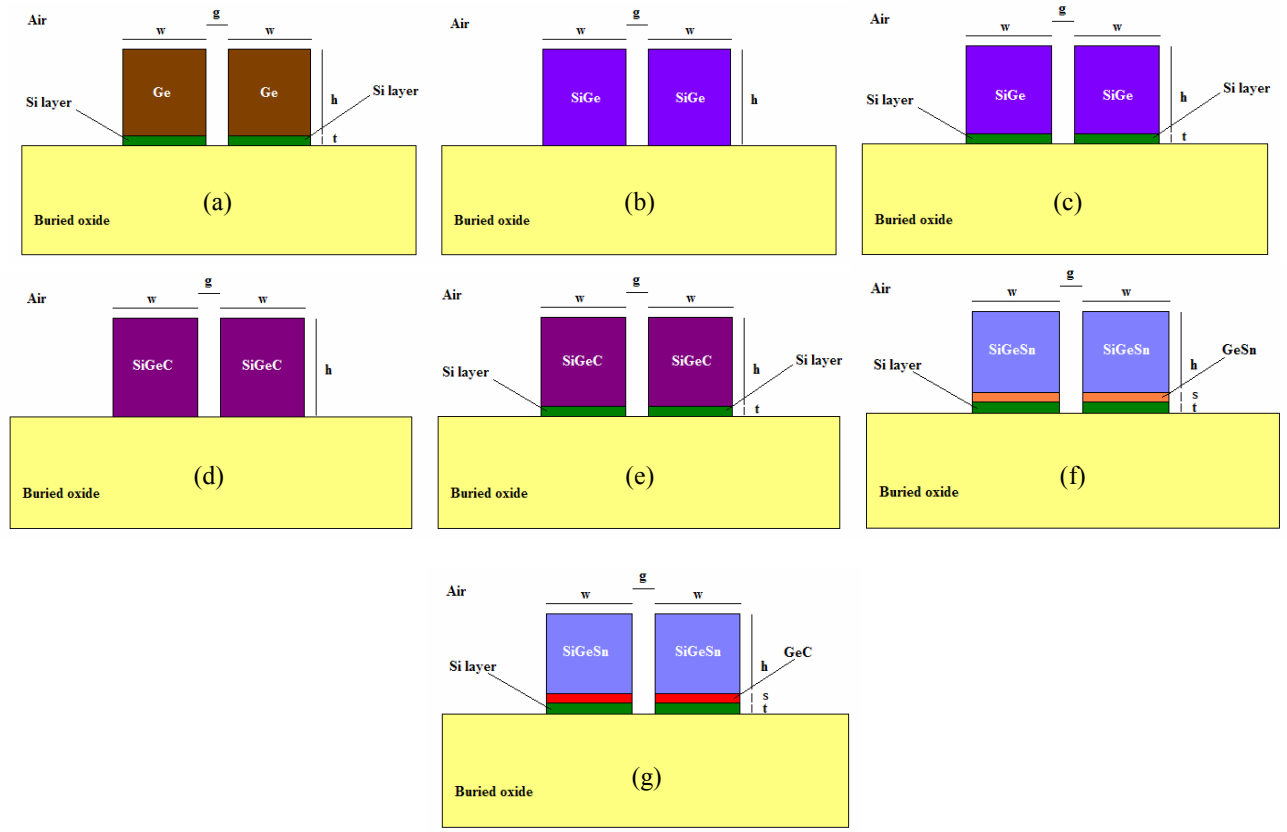

Figure 4. Novel slot optical waveguides based on group IV alloys and material systems, designed at λ = 3.39 µm.

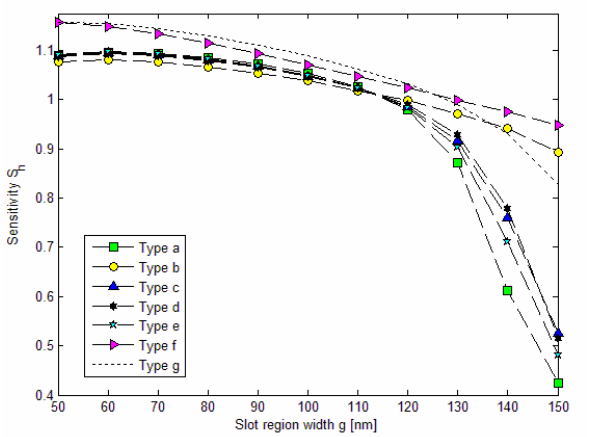

Figure 5. Sensitivity of optimized waveguides designed at 3.39 µm (quasi-TE slot mode).

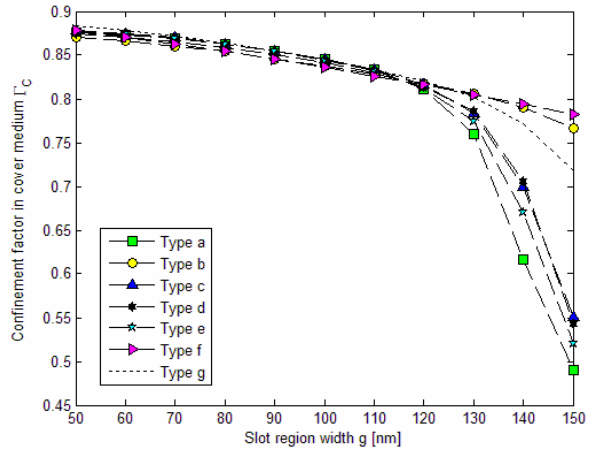

Figure 6. Confinement factor in the cover medium of optimized slot waveguides.

This means to have more relaxed sizes, without any critical technological limitation as lithographic resolution. The parametric analysis has allowed the waveguide geometrical sizes to be optimized by setting a precise value of g, simultaneously achieving very high sensitivity, large confinement factors as well as low losses. Generally, the trend of the sensitivity function can be well supported by the analysis of relevant confinement factors, as shown in Figures 6 and 7.

In fact, the waveguides exhibiting the highest Γ_C and Γ_S are still those previously indicated as (f) and (b). In both photonic devices, the percentage of the optical field in the slot region is higher than 60% for g < 140 nm. All other optimized photonic devices are characterized by a strong dependence on the slot region width. In fact for g > 140 nm, all sensitivities rapidly drop to 0.5 and 0.4. Analogous considerations can be derived for confinement factors.

 ISBN: 978-1-61208-145-8

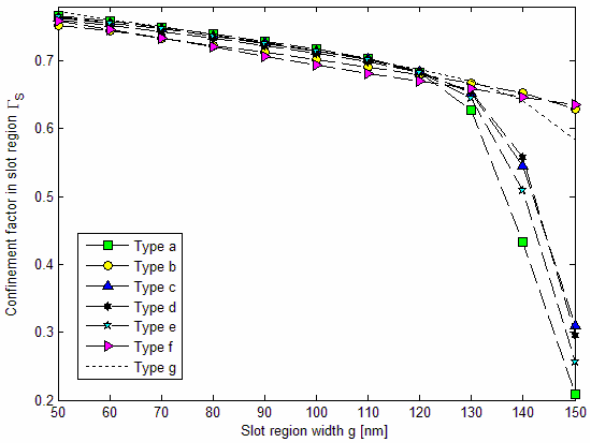

Figure 7. Confinement factor in the slot region of optimized waveguides.

V. FABRICATION TOLERANCES

All above investigated photonic structures represent an ideal case of realistic optical slot devices. In fact, vertical sidewalls characterizing slot waveguide wires are very difficult to be obtained by state of the art etching processes, for example inductively coupled plasma (ICP) etching. Thus, deviations from ideal case have to be considered and the most important parameter quantifying this effect is the tilting angle θ, as sketched in Figure 8. Thus, it is possible to distinguish between ideal and real structures, having vertical (θ = 0°) or non vertical sidewalls ($\theta \neq$ 0°), respectively.

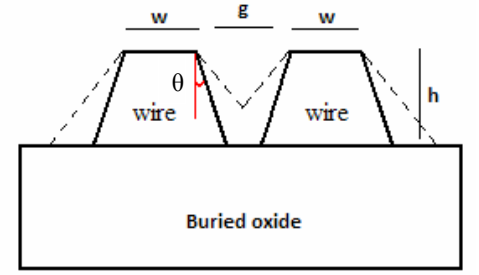

Figure 8. Schematic view of real slot waveguide.

Therefore, an analysis of real photonic structures, corrupted by fabrication characteristics, has been carried out, again in terms of homogeneous sensitivity, by choosing a specific value for the slot region width, g = 100 nm. Figure 9 shows the influence of etching tilting angle on sensitivity. All values at θ = 0° are referred to optimized ideal waveguides, whose geometrical parameters are summarized in Table II, and are also shown in Figure 5 for g = 100 nm.

Therefore, it is possible to define a critical range for the tilting angle θ, extended from 4° to 6°. In particular, a large negative slope of all sensitivity functions can be recognized in Figure 9 for these values.

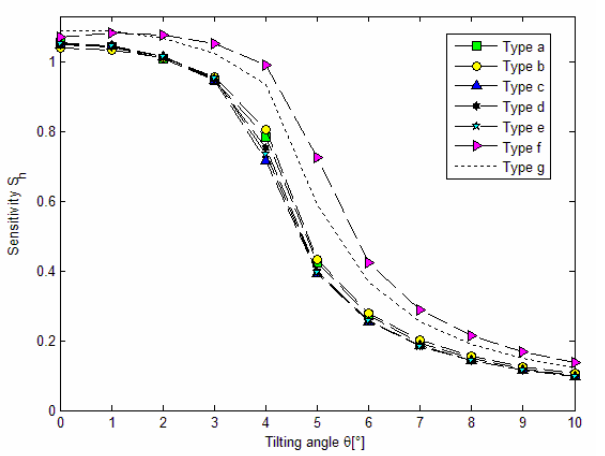

Figure 9. Sensitivity of optimized slot waveguides as a function of the tilting angle for g = 100 nm (λ = 3.39 µm).

In fact, sensitivities rapidly drop to very low values, e.g., S_h = 0.2. It is clear how this performance cannot be suitable for gas sensing because only 20 % of cover refractive index change should be detected in this case. Obviously, the smaller the parameter g, the poorer the fabrication tolerances. In addition, the thicker the slot wires, the stronger the effect of the sidewalls inclination.

The theoretical investigation on fabrication tolerances has been also carried out for calculation of confinement factors in the same way, where Γ_C and Γ_S are characterized by similar trends as a function of tilting angle θ. In conclusion, it is not possible to fabricate real photonic sensors with g = 50 nm, i.e., the lowest slot gap width allowing highest sensitivity (see Figure 5), while etching tilting angle must be limited within 4° or 5°, to avoid any corruption of sensor performance. Thus, the solution to this technological problem is strictly related with optimization of etching process for a given combination of material systems. However, standard etching processes can assure tilting angles within 1°-2°, not critical for our structures.

Moreover, these novel photonic structures are also characterized by another very important feature, i.e., the presence of a second order quasi-TE slot mode. In Figure 10 the sensitivity evaluated for the second order slot mode in all optimized structures presented in Table II, is shown as a function of g. All curves, obtained by FEM, exhibit a peak value (around 1) of sensitivity, commonly placed at g = 160 nm. For g > 160 nm, all sensitivities drop to 0.6. For values of g < 160 nm, a steep negative peak characterizes all trends, S_h quickly dropping to about 0.55. In conclusion, the presence of the second order slot-mode in optimized waveguides represents an additional technological degree of freedom in the design of these novel photonic sensors working in mid-IR. Thus, the solution to fabrication tolerance problems can be found by selecting the parameter g greater than the optimal one, in order to prevent a reduction of the slot region width due to non vertical sidewalls generated by etching process.

 ISBN: 978-1-61208-145-8

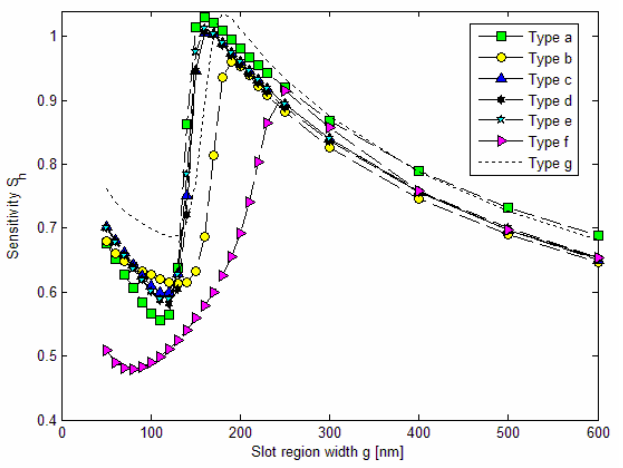

Figure 10. Sensitivity of optimized SOI slot waveguides as a function of g (second order slot-mode, λ = 3.39 µm).

In addition, confinement factors are both characterized by analytical trends similar to those of sensitivity functions. In conclusion, the choice of g = 100 nm appears to be the best suitable for both first order and second order slot-mode, simultaneously improving the fabrication tolerances. Then, relaxed dimensions of optimized waveguides will allow the fabrication of high performance multi-mode photonic devices for gas sensing applications.

In summary, novel photonic sensors proposed in this paper exhibit intriguing performances (S_h > 1). In particular, their integration in sophisticated photonic architectures, such as ring resonators, is expected to show very interesting performance in terms of wavelength shift per refractive index unit (RIU). This possibility has been also simulated and some values of wavelength sensitivity (WS) $\Delta\lambda/n_c$ are summarized in Table III for optimized structures with g = 100 nm.

TABLE III. OPTIMAL STRUCTURE WAVELENGTH SENSITIVITY IN RING RESONATOR ARCHITECTURES (g = 100 nm).

Optimal structures	WS [nm/RIU]	LOD [RIU]
Photonic crystal [1]	80	1×10^{-4}
Ring resonator [2]	140	8×10^{-5}
SOI at 1.55 µm [6]	~ 1000	8×10^{-5}
Type (a)	2050	3.90×10^{-5}
Type (b)	2126	3.76×10^{-5}
Type (c)	2126	3.76×10^{-5}
Type (d)	2111	3.79×10^{-5}
Type (e)	2115	3.78×10^{-5}
Type (f)	2194	3.64×10^{-5}
Type (g)	2128	3.76×10^{-5}

A comparison with some results in literature, both experimental and theoretical, can be observed. Thus, huge wavelength shifts as large as 2200 nm/RIU, which cannot be achieved by other photonic architectures, could be exploited in ring resonators based on these optimized photonic slot structures, realized with an appropriate combination of group IV materials and alloys. Since a wavelength resolution as low as 80 pm is practical in ordinary optical spectrum analyzers, a limit of detection as low as 3.6×10^{-5} RIU could be obtained in these powerful photonic structures, able to detect very small volumes of gas traces in mid-IR, of the order of 1 µm^3.

VI. CONCLUSION AND FUTURE WORK

In this paper, intriguing novel photonic sensors have been investigated in detail by a FEM approach. In particular, unconventional group IV alloys and material systems have been adopted for design of ultra-high performance photonic gas sensors working in mid-IR. Appropriate combinations of group IV compounds have been chosen on the basis of their technological compatibility and low losses in mid-IR wavelength range. Optimized photonic slot structures are characterized by relaxed dimensions allowing large margins of fabrication tolerances. In addition, the presence of a second order slot-mode has been also demonstrated, giving further flexibility in design. In conclusion, optimized slot waveguides for efficient sensing in mid-IR exhibit much higher performance with respect to SOI slot devices designed at near-IR (1.55 µm), with an improvement of more than 110%. Further work on this topic will be devoted to detailed model and design of slot-based ring resonators constituted by several combinations of group IV materials and alloys, with the aim to further improve the performance of photonic sensors in mid-IR and their use in several application fields.

REFERENCES

[1] T. Sunner, T. Stichel S.-H. Kwon, T. W. Schlereth, S. Holfing, M. Kamp, A. Forchel "Photonic crystal cavity based gas sensor," Appl. Phys. Lett., Vol. 92, n. 26, 2008, art. 261112.

[2] V. M. N. Passaro, F. Dell'Olio, and F. De Leonardis, "Ammonia Optical Sensing by Microring Resonators," Sensors, Vol. 7, n. 11, 2007, pp. 2741-2749.

[3] X. Fan, I. M. White, S. I. Shopova, H. Zhu, J. D. Suter, Y. Sun, "Sensitive optical biosensors for unlabeled targets: A review," Analytica Chimica Acta, Vol. 620, 2008, pp. 8-26.

[4] V. M. N. Passaro, F. Dell'Olio, C. Ciminelli, and M. N. Armenise, "Efficient Chemical Sensing by Coupled Slot SOI Waveguides," Sensors, Vol. 9, n. 2, 2009, pp. 1012-1032.

[5] P. Bienstman, K. De Vos, T. Claes, P. Debackere, R. Baets, J. Girones, E. Schacht, "Biosensors in Silicon on Insulator," Proc. SPIE on Silicon Photonics IV, Vol. 7220, 2009, art. 72200N.

[6] F. Dell'Olio, and V. M. N. Passaro, "Optical sensing by optimized silicon slot waveguides," Opt. Express, Vol. 15, n. 8, 2007, pp. 4977-4993.

[7] Comsol Multiphysics by COMSOL, Stockholm, ver. 3.2, single license, 2005.

[8] M. Iqbal, Z. Zheng, and J. S. Liu, "Light confinement in multiple slot structures investigated," Proc. IEEE Int. Conf. on Microwave and Millimiter Wave Technol. (ICMMT), 2008, pp. 878-891.

[9] R. Soref, S. J Emelett, and W. R Buchwald, "Silicon waveguided components for the long-wave infrared region," J. Opt. A: Pure Appl. Opt., Vol. 8, 2006, pp. 840-848.

 ISBN: 978-1-61208-145-8